

MORPHOLOGY SEGREGATION OF GALAXIES IN THE COLOR-COLOR GRADIENT SPACE

CHANGBOM PARK^{1,2} AND YUN-YOUNG CHOI^{1,3}*Draft version July 16, 2018*

ABSTRACT

We have found the $u - r$ color versus $g - i$ color gradient space can be used for highly successful morphology classification of galaxies in the Sloan Digital Sky Survey. In this space galaxies form early and late type branches well-separated from each other. The location of galaxies along the branches reflects the degree and locality of star formation activity, and monotonically corresponds to the sequence of morphological subclasses. When the concentration index is used together, the completeness and reliability of classification reaches about 91% for a training set of SDSS galaxies brighter than $r_{\text{pet}} \approx 15.9$. At faintest magnitudes ($r_{\text{pet}} \approx 17.5$) of the SDSS spectroscopic sample, the performance still remains at about 88%. The new classification scheme will help us find accurate relations of galaxy morphology with spatial and temporal environments, and help one understand the origin of morphology of galaxies.

Subject headings: galaxies: fundamental parameters

1. INTRODUCTION

Unlike stars, galaxies show diverse shapes. The belief that the difference in appearance reflects the generic character has motivated morphological classification of galaxies. Since the 1920s the simple scheme suggested by Hubble (Hubble 1926) based on single band images of bright galaxies has been widely adopted. The essence of Hubble's scheme and its elaborations (De Vaucouleurs et al. 1991; Kormendy 1979; De Vaucouleurs 1959; Sandage 1961) is to divide galaxies into early and late types. The early types are further divided into ellipticals and lenticulars, and the late types into spirals (unbarred and barred) and irregulars. Any one who looks directly into galaxy images immediately realize that shapes of galaxies are much more diverse than this, but also that the simple Hubble sequence catches the major features of galaxy morphology. As unprecedentedly large sets of digital images of galaxies such as the Sloan Digital Sky Survey (SDSS, full details of the SDSS are available at <http://www.sdss.org>. York et al. 2000) data are available, time is ripe for understanding the origin of morphology of galaxies. In order to find the accurate relationship of galaxy morphology with other physical properties it is required to define morphological types more objectively and to use morphology subsets as homogeneous as possible. The endeavors to develop an objective, automatic and highly successful morphology classifier applicable to large libraries of digital images have resulted in various schemes (Yamauchi et al. 2005; Blanton et al. 2003a; Abraham, van den Bergh, & Nair 2003; Strateva et al. 2001; Shimasaku et al. 2001; Abraham et al. 1996; Doi, Fukugita, & Okamura 1993). This work further advances this topic.

The philosophy of our morphological classification is to develop a scheme applicable down to the faint magnitude limit ($r_{\text{pet}} \approx 17.77$ where r_{pet} is the Petrosian magnitude after Galactic extinction correction) of the

spectroscopic sample of the SDSS using only photometric information. The fundamental features of galaxy morphology still useful for galaxies near the faint limit are the surface brightness and color profiles. Their mean levels are measured by mean surface brightness and integrated color. Their radial variation scaled to a characteristic size can be measured by the Sersic or concentration index, and color gradient, for example. Therefore, in principle, the morphology classification of galaxies should be made at least in 4-dimensional parameter space. The surface brightness at long wavelength bands represents the stellar mass distribution, and the color tells about the recent star formation history. A difficulty in dividing galaxies into early and late types using the surface brightness profile alone lies in the fact that most spirals consist of both bulge and disk. There is an unavoidable confusion between the bulge-only and the bulge-plus-disk systems when only the surface brightness information in a single band is used for classification. Contamination in the early and late type subsets separated by using the concentration index, for example, is typically about 20% (Yamauchi et al. 2005; Shimasaku et al. 2001). The surface texture is of limited usage because it is sensitive to seeing and is simply lost for small faint galaxies ($r_{\text{pet}} > 16.0$ in the case of SDSS; Yamauchi et al. 2005). On the other hand, the information in color reveals the additional generic difference between early and late type galaxies which have experienced different star formation histories. Strateva et al. (2001) has found that the integrated (observer frame) $u^* - r^*$ color (asterisks are attached to the SDSS photometry based on the photometric equations used through the Early Data Release) of the SDSS Main galaxies (Stauss et al. 2002) shows a bimodal distribution. However, they have shown that, when divided at $u^* - r^* = 2.22$, the early (E/S0/Sa) and late type (Sb/Sc/Irr) subsets have significant contaminations reaching about 30% for a sample with visually identified morphological types. In this paper we extend their work by incorporating color gradient and the concentration index as additional dimensions of the classification parameter space.

¹ Korea Institute for Advanced Study, Dongdaemun-gu, Seoul 130-722² cbp@kias.re.kr³ yychoi@kias.re.kr

2. THE TRAINING SAMPLE

We use a training set of 1982 galaxies to quantify the performance of our morphology classification scheme. The training set consists of two samples. The first contains 981 SDSS galaxies with $14.5 < r_{\text{pet}} \leq 15.0$ after Galactic extinction correction whose morphological types are assigned by the authors based on the color images retrieved by the SDSS Image List Tool (<http://cas.sdss.org/astro/en/tools/chart/list.aspx>). Galaxies are divided into six types: E/S0 (smooth brightness and color profile), S0 (disk with features, but no spiral arm), AE (E or S0 with abnormal brightness or color distribution), S (spiral arm, disk with dust lane), AS (spirals with large distortion in shape), I (irregulars). The first three correspond to the early type, and the rest is the late types. The second training set is Fukugita et al.'s catalog (in preparation; see also Nakamura et al. 2003) listing 1,875 galaxies with $r_{\text{pet}}^* \leq 15.9$ (after Galactic extinction correction) and with visually identified morphological types from $T = 0$ to 6 at half integer steps. Among them we use a subset of 1183 galaxies that are listed both in the Main Galaxy and the spectroscopic sample and are not too much contaminated by foreground stars. By comparing the morphological types of 182 galaxies common in our sample and Fukugita et al.'s catalog, we have found that the early and late types divide at $T = 1.5$ ($T = 1$ and 2 correspond to Hubble Type S0 and Sa, respectively) in the latter catalog.

3. MORPHOLOGY CLASSIFICATION SCHEME

We use the color versus color gradient space as the major morphology classification tool, and use the concentration index as an auxiliary parameter. In the color-color gradient space spirals tend to separate from the region clustered by ellipticals and lenticulars as majority of spirals exhibit significant color gradient. As a measure of color gradient, we adopt the difference in ${}^{0.1}(g-i)$ color of the region with $R < 0.5R_{\text{pet}}$ from that of the annulus with $0.5R_{\text{pet}} < R < R_{\text{pet}}$, where R_{pet} is the Petrosian radius and ${}^{0.1}(g-i)$ is a rest frame $g-i$ color K -corrected to the redshift of 0.1 (hereafter, $g-i$ means ${}^{0.1}(g-i)$), and K -correction of magnitude and color is calculated based on the study of Blanton et al. (2003b). Negative color difference means bluer outside. Model magnitude is used for color. It is the magnitude calculated from the best-fit model profile obtained by fitting the de Vaucouleur and exponential profiles to the galaxy image. We have chosen the g - and i -bands to estimate color gradient because they are widely separated in wavelength across the 4,000-Å break, and have S/N ratios higher than the u - and z -bands. Choice of other bands results in nosier color gradient estimates at faint magnitudes, or less successful separation of galaxies into early and late types. Other measures of color gradient like the linear slope of the radial $g-i$ color profile and the $g-i$ color difference between the region with $R < R_{50}$ and the annulus with $R_{50} < R < R_{90}$, are also calculated for comparisons. R_{50} and R_{90} are the radii from the center of a galaxy containing 50 and 90% of the Petrosian flux. We have found that the clump of the normal early type galaxies in the color-color gradient space is less tight for the latter measures at fainter magnitudes $r_{\text{pet}} > 16$.

Throughout this paper we use AB magnitudes con-

verted from SDSS magnitudes. The g - and i -band atlases images and basic photometric parameters of individual galaxies are retrieved from the SDSS Data Release 3 (DR3) at Princeton (<http://photo.astro.princeton.edu>). We have generated a big set of Sersic model images convolved with the PSF of various sizes. These images are used to find a best-fit Sersic model with true Sersic index and true axis ratio for an observed image of a given size of the PSF. The fitting is made at radii larger than $0.2R_{\text{pet}}$ to avoid the central region whose profile is much affected by seeing. Then the best-fit Sersic models in g - and i -bands are convolved with the PSF of the same size, and the effects of seeing on the concentration index and color difference are estimated. We have confirmed the seeing-corrected concentration index and color difference show no apparent dependence on seeing. We use the elliptical annuli in all our parameter calculations to take into account flattening or inclination of galaxies. The position angle and axis ratio used to define the elliptical annuli and to calculate the radial surface brightness profile are isophotal ones measured from the i -band image. The Petrosian radii in our analysis are usually larger than those in the DR3 catalog which adopted circular annuli.

The photometric parameters we use for morphology classification are the $u-r$ color, color difference $\Delta(g-i)$, and the (inverse) concentration index c in the i -band, where $c \equiv R_{50}/R_{90}$. Here, the concentration index is used as a complementary parameter to discriminate red disk spirals from early type galaxies. The i -band image is used to measure the index because the image at longer wavelengths is expected to better represent the stellar mass distribution. All parameters are seeing-corrected as described above.

Figure 1 shows the distribution of galaxies of this training set in the $u-r$ versus $\Delta(g-i)$ space and in the $u-r$ versus concentration index space. The early (E/S0) and late types (Sa to Sd) determined by visual inspection are marked as circles (red) and crosses (blue), respectively. Squares (green) are irregulars. In our automated scheme classified as early type galaxies are those lying above the boundary lines passing through the points (3.5, -0.15), (2.6, -0.15) and (1.0, 0.3) in the $u-r$ versus $\Delta(g-i)$ space. They are also required to have $c < 0.43$. The rest are classified as late types. The completeness of this classification scheme reaches 91.3% for early types and 90.1% for late types. The reliabilities are 90.1% and 91.4%, respectively. The completeness, C , is the fraction of galaxies of a given type that are successfully selected from the original sample by the classification scheme. The reliability, R , is the fraction of galaxies of the desired type from the selected subsample. The 9 ~ 10% failure is due to a few red passive spirals, galaxies with companions or foreground stars, and to incorrect visual classification (for edge-on objects in particular). The parameter c does only an auxiliary role improving the results by a few percents.

We estimate the completeness and reliability of our morphology classification is about 88% near $r_{\text{pet}} = 17.5$, which is close to the faint end of the spectroscopic sample of the SDSS. The performance of our classification scheme slowly degrades at $r_{\text{pet}} \geq 16$ because it becomes harder to measure the color difference and concentration index as the size of galaxies relative to the CCD pixel and the FWHM of the PSF decreases. To estimate

the performance of our classification scheme at fainter magnitudes we redshift the galaxies in the training sample ($r_{\text{pet}} = 14.5 \sim 15.0$) with morphological types assigned by us. We calculate the new redshift at which a galaxy appear dimmer by a desired magnitude adopting a cosmology with density parameters $\Omega_m = 0.27$ and $\Omega_\Lambda = 0.73$. The reduction factor in angular size is calculated and images are binned down (Giavalisco et al. 1996). The resulting images are convolved with the PSF in such a way that they have the seeing effects equal to those of the original ones. Noises are not added anew. Following this procedure we generated three mock morphology samples of 981 galaxies in half magnitude bins from $r_{\text{pet}} = 16.0$ to 17.5. The distributions of these redshifted galaxies in the color-color gradient space and in the color-concentration index space are very similar with those of three samples of randomly-drawn 1,000 SDSS galaxies with actual magnitudes in the same bins, thus justifying our procedure. We determine the classification criteria at fainter magnitudes using these redshifted morphology samples. Results are summarized in Table 1. Table 1 says that our classification boundaries in the color-color gradient space hardly change even at magnitudes down to $r_{\text{pet}} = 17.5$. The only major change is the boundary at the reddest colors (the line connecting to the point P3). At fainter magnitudes the clump of the normal E/S0's expands vertically in the color-color gradient space because the measured color-differences have more errors. The classification boundary at the reddest colors has been chosen to include more ellipticals taking into account this fact. We think the K -correction of color in this reddest color range has been accurately estimated. Our K -correction might have more errors for intermediate-type spirals for which the spectra of the central part of galaxies are less representative of the total color. But in this case our classification is hardly affected because these galaxies are blue, have large color gradients, and are located far from the classification boundaries.

4. DISCUSSION

Inspection of location of galaxies in the color-color gradient space leads us to classification beyond the dichotomous division into early and late types. Normal ellipticals and lenticulars are very homogeneous systems whose light is dominated by old Population II stars. They strongly concentrate within a spot centered at $(2.82, -0.04)$ in the $u - r$ and $\Delta(g - i)$ plane. Dispersion is mainly due to companions or foreground stars. They show very weak but definite color gradient (i.e., outside is bluer). We have discovered a trail of early types containing about 10% of early type galaxies toward the left hand direction ($u - r < 2.5$) from the concentration of normal early types and then upwards. The galaxies in this trail are bluer than normal ones, often show emission lines, and occasionally show star burst activity near the center. They tend to be more centrally concentrated than spirals at the same color. We have found that most $E+A$ galaxies (Dressler & Gunn 1983) listed in Yamauchi & Goto (2005) are located in this trail.

On the other hand, a spiral branch is extended downward of the cluster of normal early types. Sa type spirals often start to have star forming zones at the outskirt of disk. Their integrated color is still dominated by the red light from their bulges, but they begin to show color gradient. As the star formation activity becomes stronger, color gradient increases first and then starts to decrease as the star forming region expands toward the center. Very late type spirals and most irregulars at the upper left corner are very blue and have inverted color gradient (i.e., center is bluer) since they usually show strong star burst near the center. The spiral branch meets the trail of early types there. The major advantage of morphology classification in the color-color gradients space is that the blue early type galaxies are separated from the spiral galaxies because the former tend to have nearly constant color profile or bluer cores while the latter tend to have red bulge plus blue disk structure. The spiral branch is a sequence of locality of star formation activity and cold gas and dust concentration as illustrated in Fig. 2. The position of a spiral along the branch has a strong correlation with its morphological subclass as shown in Fig. 3. After making early-late type division, one can further divide galaxies into subclasses based on their location along the early and late type branches. For example, late type galaxies can be divided into $L1$, $L2$, and $L3$ subclasses which group galaxies lying above the line $\Delta(g - i) = 0.8 - 0.4(u - r)$, between this line and the line $\Delta(g - i) = 1.6 - (u - r)$, and left of the latter line, respectively. These subclasses roughly correspond to Sa-Sb, Sb-Sc, and Sc-Sd/Irr, respectively. Dispersion of the spiral branch is partly due to internal extinction which tends to make $u - r$ and $|\Delta(g - i)|$ increase. Dependences of $u - r$ and $|\Delta(g - i)|$ on axis ratio of galaxies indicate that the effects of internal extinction are strongest for intermediate type spirals.

Our new morphology classification scheme takes into account history and locality of star formation as well as stellar mass distribution. It is easy to implement the scheme for multi-band surveys with wide spectrum coverage. We expect that the strong concentration of early types and the general shape of the spiral branch in the color versus color gradient space are still maintained for galaxies at high redshifts. Any change in their location and shape will be colorful evidence for evolution of star formation activity and cold gas infall into galaxies with different morphology.

CBP thanks Michael Vogeley for collaboration on parts of this work and for invitation to Drexel University when this work was started. We also thank Yasushi Suto for suggesting us to use Fukugita et al.'s catalog. We thank the anonymous referee for helpful comments. This work is supported by the Korea Science and Engineering Foundation (KOSEF) through the Astrophysical Research Center for the Structure and Evolution of Cosmos (ARCSEC).

REFERENCES

- Abraham, R. G., et al. 1996, ApJS, 107, 1
 Abraham, R. G., van den Bergh, S., & Nair, P. A. 2003, ApJ, 588, 218
 Blanton, M. R., et al. 2003a, ApJ, 594, 186
 Blanton, M. R., et al. 2003b, AJ, 125, 2348
 De Vaucouleurs, G. 1959, Handbuch der Physik, 53, 275

- De Vaucouleurs, G., et al. 1991, in *Third Reference Catalogue of Bright Galaxies*, (New York: Springer)
- Doi, M., Fukugita, M., & Okamura, S. 1993, MNRAS, 264, 832
- Dressler, A., & Gunn, J. E. 1983, ApJ, 270, 7
- Giavalisco, M., Livio, M., Bohlin, R. C., Macchetto, F. D., & Stecher, T. P. 1996, AJ, 112, 369
- Hubble, E. P. 1926, ApJ, 64, 321
- Kormendy, J. A. 1979, ApJ, 227, 714
- Nakamura, O., et al. 2003, AJ, 125, 1682
- Sandage, A. 1961, in *The Hubble Atlas of Galaxies* (Washington: Carnegie Institution)
- Shimasaku, K., et al. 2001, AJ, 122, 1238
- Stoughton, C., et al. 2002, AJ, 123, 485
- Strateva, I., et al. 2001, AJ, 122, 1861
- Strauss, M. A. 2002, AJ, 124, 1810
- Yamauchi, C., & Goto, T. 2005, MNRAS, 359, 1557
- Yamauchi, C., et al. 2005, MNRAS(in press)
- York, D., et al. 2000, ApJ, 120, 1579

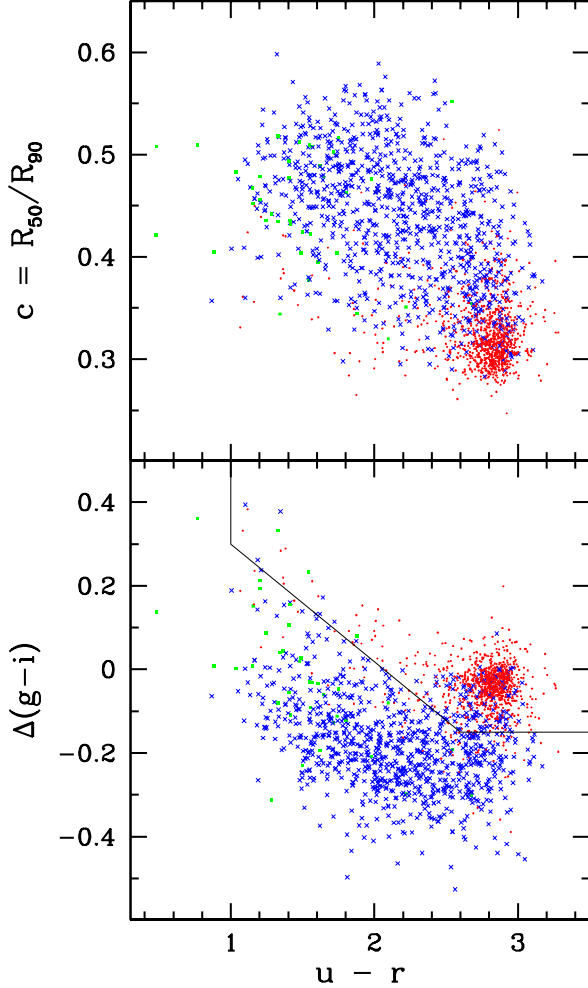


FIG. 1.— Distributions of the 1982 galaxies in the morphology training set in the $u - r$ color versus the (inverse) concentration index space (upper panel) and in the $u - r$ color versus the $\Delta(g - i)$ color difference space (lower panel). Red dots are early types (E/S0, S0, AE), blue crosses are spirals (S, AS), and green squares are irregulars (I).

TABLE 1
CLASSIFICATION CRITERIA

Magnitude bins	14.5 ~ 16.0	16.0 ~ 16.5	16.5 ~ 17.0	17.0 ~ 17.5
Classification Criterion Parameters				
$P1$	(1.00, 0.30)	(1.00, 0.30)	(1.00, 0.30)	(1.00, 0.30)
$P2$	(2.60, -0.15)	(2.65, -0.18)	(2.65, -0.18)	(2.70, -0.18)
$P3$	(3.50, -0.15)	(3.50, -0.15)	(3.50, -0.25)	(3.50, -0.35)
c_{cut}	0.43	0.45	0.47	0.48
Completeness (C) and Reliability (R)				
C(Elliptical)	0.913	0.883	0.872	0.883
R(Elliptical)	0.901	0.892	0.882	0.881
C(Spiral)	0.901	0.902	0.892	0.890
R(Spiral)	0.914	0.893	0.883	0.892

The three points, $P1$, $P2$, and $P3$, define the lines dividing the SDSS galaxies into the early and late types in the $u - r$ versus $\Delta(g - i)$ plane. The early types are also required to have $c < c_{cut}$.

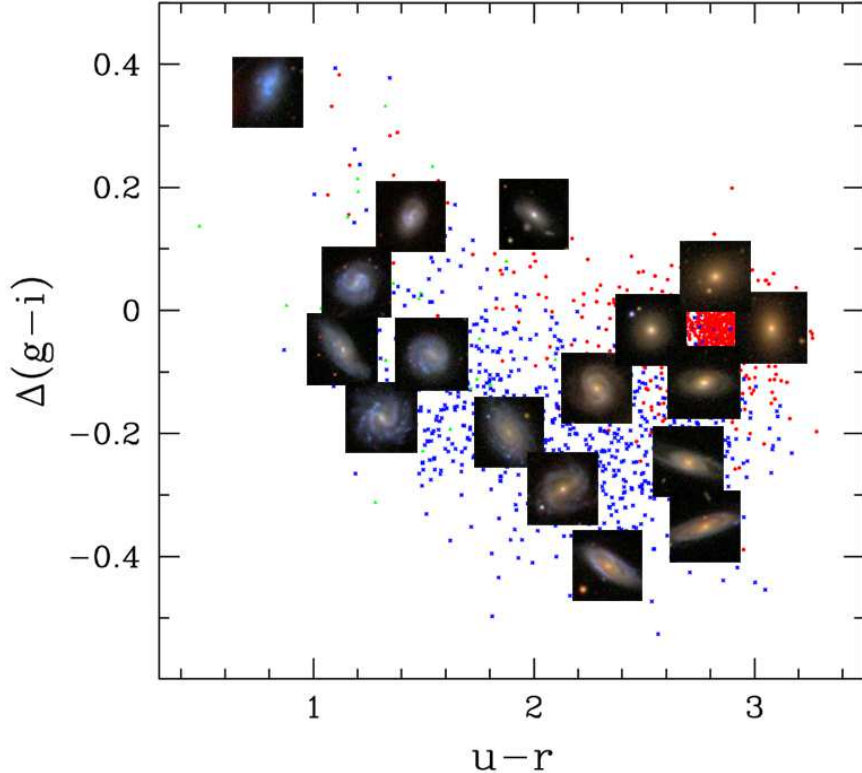


FIG. 2.— A picture showing the continuous changes in the appearance of galaxies along the spiral and elliptical branches. Note that the star forming region extends from the outskirt of disk toward the center as one moves from red to blue spirals.

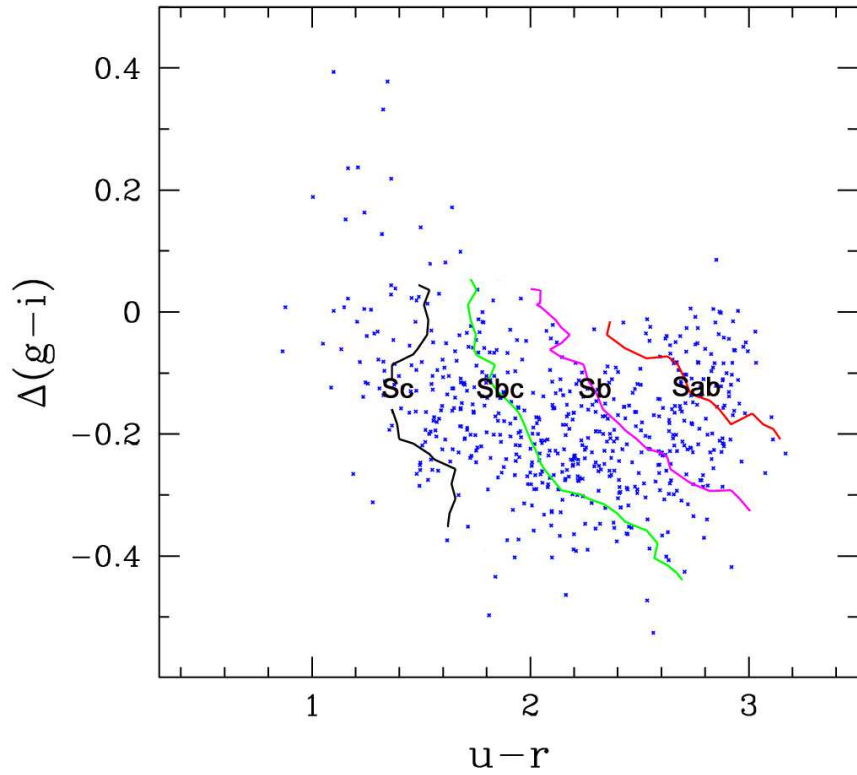


FIG. 3.— Distribution in the $u - r$ color versus the $\Delta(g - i)$ plane of 582 spiral galaxies in the training set taken from Fukugita et al.'s morphology sample which lists subclasses for spirals. Superposed are the iso-subclass contours calculated by averaging the listed subclasses within the ellipse of axis lengths of 0.6 and 0.2 in the $u - r$ and the $\Delta(g - i)$ directions, respectively. Contour levels are $T = 2.5$ (Sab), 3 (Sb), 3.5 (Sbc), and 4 (Sc) from right to left.